완전 연동된 수리지질역학적 모델을 이용한 사면 내의 지하수유동과 사면의 안정성에 대한 강수의 영향 평가

Evaluation of Rainfall Impacts on Groundwater Flow in Slopes and Slope Stability Using a Fully Coupled Hydrogeomechanical Model

김준모, Jun-Mo Kim

서울대학교 지구환경과학부 조교수, Assistant Professor, School of Earth and Environmental Sciences, Seoul National University

개 요 : 강수량 변동에 따른 사면 내의 지하수유동과 사면의 안정성 변화를 동시에 분석·평가하기 위하여 하나의 완전 연동된 수리지질역학적 모델을 제시하였다. 이 모델은 변형성 지질매체 내에서의 지하수유동을 설명하는 일련의 지배식들과 Galerkin 유한요소법에 기초하여 개발되었다. 1990년부터 1999년까지의 서울지역의 건기 (1월) 및 우기 (8월) 강수량 하에 있는 토양 사면에 대해 개발된 모델을 적용하여 일련의 수치실험을 실시하였다. 수치실험의 결과는 강수량이 증가함에 따라 사면의 수리역학적 안정성이 전반적으로 악화됨을 보여준다. 즉 강수량이 증가할수록 공극수압이 증가하고 지하수면이 상승한다. 그 결과 불포화대가 축소되고 삼출면이 팽창되며 사면의 전단부를 따라 지하수유동속도가 증가하게 된다. 동시에 강수량이 증가할수록 사면 전단부를 향해 전반적인 변위량이 증가한다. 그 결과 안전율이 1 이하인 불안전한 지역이 사면 전단부에서 사면 상부 쪽으로 전파·팽창되며 그 두께도 증가한다. 수치실험의 결과는 또한 사면의 표면에서는 전단파괴와 더불어 인장파괴도 발생할 수 있음을 보여준다.

Key words : rainfall, groundwater flow, slope stability, poroelasticity theory, finite element modeling

1. Introduction

In recent years around the world, rainfall-induced slope instability in variably saturated soils and loose fills has attracted increasing concern and attention not only from the general public but also from geoscientists and civil engineers because of the uniqueness of its mechanism. Intensive rainfall, which acts as a hydraulic stress, intrinsically induces the hydromechanical interaction between the groundwater flow field and the solid skeleton (medium) deformation field within a geologic medium as follows. As infiltration of rainfall into a slope takes place, the pore water pressure increases and the groundwater table rises causing a reduction in the matric suction, an expansion of the seepage face, and an increase in the groundwater velocity. This, in turn, leads to a decrease in the effective stress acting on the solid skeleton causing a decrease in the shear strength on the potential failure surface to a point where equilibrium can no longer be sustained in the slope and then failures may occur. This hydrogeomechanical phenomenon can be better explained through the fully coupled poroelasticity theory than by the conventional theory of solid skeleton deformation that is uncoupled from groundwater flow. Since the pioneering work of Biot (1941), the poroelasticity theory has been extensively developed for variably saturated anisotropic porous and fractured geologic media.

A series of two-step numerical approaches has been presented to evaluate effects of infiltration on

the stability of variably saturated slopes (Cai *et al.*, 1998; Ng and Shi, 1998; Fourie *et al.*, 1999). In their approaches, the spatial distribution of the pore water pressure is first obtained independently by solving a simple variably saturated water flow equation in terms of the pore water pressure only using a finite element method. It is then used as an input groundwater condition to determine the factor of safety using a limit equilibrium method. Thus, in their approaches, the groundwater flow field and the solid skeleton deformation field are actually uncoupled. On the other hand, a linear poroelastic numerical model has been developed to analyze the relationship between groundwater flow and slope stability (Iverson and Reid, 1992; Reid and Iverson, 1992). However, in their model, it is assumed that the slopes are fully saturated with water. Thus, using their model, one cannot investigates rainfall impacts on groundwater flow and slope stability under the unsaturated flow condition and the variable rainfall-infiltration-seepage slope surface, which are more realistic.

The objectives of this paper are thus to present a general fully coupled hydrogeomechanical model and to quantitatively analyze the rainfall impacts on variably saturated groundwater flow and slope stability, as an important application of the nonlinear poroelasticity theory. From a practical point of view, a quantitative understanding of such rainfall impacts may provide more improved guidelines for predicting the slope instabilization and failure and maintaining the slope stability required.

2. Governing Equations

The poroelastic governing equations for groundwater flow in deforming variably saturated porous geologic media may be written as (Kim and Parizek, 1999a; Kim and Parizek, 1999b; Kim, 2000)

$$\nabla \cdot [-\boldsymbol{K} \cdot (h+z)] + \left(n\frac{dS_w}{dh} + n\, S_w\, \beta_w\, \gamma_w\right)\frac{\partial h}{\partial t} + \alpha_c\, S_w \frac{\partial}{\partial t}\left(\frac{\partial u_k}{\partial x_k}\right) = q \tag{1}$$

$$-\frac{\partial}{\partial x_j}\left[G\left(\frac{\partial u_i}{\partial x_j} + \frac{\partial u_j}{\partial x_i}\right) + \lambda\left(\frac{\partial u_k}{\partial x_k}\right)\delta_{ij} - \alpha_c\, S_w\, \gamma_w h\, \delta_{ij}\right]$$
$$+ [n\, S_w\, \rho_w + (1-n)\, \rho_s]\, g_i = 0 \qquad i,j = x,y,z \tag{2}$$

In equation (1), $\boldsymbol{K} = K_r\, \boldsymbol{K}_{sat}$ is the effective hydraulic conductivity tensor, $h = P/\gamma_w$ is the (pore water) pressure head, z is the vertical axis and elevation head, n is the porosity, S_w is the degree of water saturation, β_w is the compressibility of water (4.4×10^{-10} m^2/N), $\gamma_w = \rho_w g$ is the unit weight of water (9.806×10^3 N/m^3), $\alpha_c = 1 - K/K_s$ is Biot's hydromechanical coupling coefficient or the effective stress coefficient, u_k is the displacement of solid in the k direction, q is the water source or sink term, and t is time. Here K_r is the relative hydraulic conductivity, $\boldsymbol{K}_{sat}$ is the saturated hydraulic conductivity tensor, P is the pore water pressure (positive for compression), ρ_w is the density of water, g is the gravitational acceleration constant, K is the bulk modulus of the solid skeleton, and K_s is the bulk modulus of solid. Note that $\phi = h + z$ is the total hydraulic head, dS_w/dh is the specific water saturation capacity, $\theta_w = n\, S_w$ is the water content, and $\varepsilon_v = \partial u_k/\partial x_k$ is the volumetric strain. In addition, $\boldsymbol{q}_r = -\boldsymbol{K} \cdot \nabla(h+z)$ is the Darcy velocity in which $\nabla(h+z)$ is the hydraulic gradient.

In equation (2), $G = \mu = E/2(1+\nu)$, $\lambda = E\nu/(1+\nu)(1-2\nu)$, G is the shear modulus, E is

Young's modulus, and ν is Poisson's ratio. The pair of constants λ and μ are often referred to as Lamé's constants. Here δ_{ij} is Kronecker's delta, ρ_s the solid density, and g_i is the component of gravitational acceleration in the i direction. In the first square bracket on the left-hand side of equation (2), the sum of the first two terms is equal to the deformation-producing incremental effective stress tensor σ'_{ij} (positive for tension), and the sum of all three terms is equal to the incremental total stress tensor σ_{ij} (positive for tension) such that $\sigma_{ij} = \sigma'_{ij} - \alpha_c S_w \gamma_w h \delta_{ij}$. The remaining term on the left-hand side of equation (2) represents the body force f_i in the i direction.

In summary, equations (1) and (2) constitute a set of four nonlinear partial differential equations with four dependent variables h, u_x, u_y, and u_z in Cartesian coordinates (x, y, z). Thus full coupling between the groundwater flow field and the solid skeleton deformation field in partially saturated porous geologic media can be achieved by simultaneously solving these governing equations with appropriate constitutive relationships for the unsaturated flow condition.

3. Numerical Formulation

The Galerkin finite element method (Istok, 1989; Lewis and Schrefler, 1998) is chosen here to approximate the governing equations (1) and (2) and to obtain their simultaneous solutions because of its practical ability to treat variably saturated heterogeneous and anisotropic regions with complex boundaries. In the finite element method, an unknown variable φ, which represents the pressure head h and the displacements u_x, u_y, and u_z in equations (1) and (2), can be approximated by a trial solution φ' in space by means of the basis (shape) functions and their nodal values as

$$\varphi(x,y,z,t) \approx \varphi'(x,y,z,t) = \sum_{J=1}^{NN} N_J(x,y,z)\,\varphi_J(t) \qquad \varphi = h,\ u_x,\ u_y,\ u_z \tag{3}$$

where N_J is the basis function for node J, φ_J is the value of the unknown variable φ at node J, and NN is the total number of nodes in a region of interest. Application of Galerkin's principle and Green's theorem and substitution of equation (3) to equations (1) and (2) yields

$$\int_R \nabla N_I \cdot \boldsymbol{K} \cdot \nabla N_J dR\{h\} + \int_R N_I \left(n \frac{dS_w}{dh} + n S_w \beta_w \gamma_w \right) N_J dR\left\{ \frac{\partial h}{\partial t} \right\}$$

$$+ \int_R N_I \alpha_c S_w \frac{\partial N_J}{\partial x_k} dR\left\{ \frac{\partial u_k}{\partial t} \right\} = \int_B N_I \boldsymbol{n} \cdot [\boldsymbol{K} \cdot \nabla (h+z)] dB$$

$$+ \int_R N_I q\, dR - \int_R \nabla N_I \cdot \boldsymbol{K} \cdot \nabla z dR \qquad I,J = 1,2,3,\cdots,NN \tag{4}$$

$$\int_R \frac{\partial N_I}{\partial x_j} G \frac{\partial N_J}{\partial x_j} dR\{u_i\} + \int_R \frac{\partial N_I}{\partial x_j} G \frac{\partial N_J}{\partial x_i} dR\{u_j\} + \int_R \frac{\partial N_I}{\partial x_j} \lambda \delta_{ij} \frac{\partial N_J}{\partial x_k} dR\{u_k\}$$

$$- \int_R \frac{\partial N_I}{\partial x_j} \alpha_c S_w \gamma_w \delta_{ij} N_J dR\{h\} = \int_B N_I \sigma_{ij} n_j dB + \int_R N_I [n S_w \rho_w + (1-n) \rho_s] g_i dR$$

$$I,J = 1,2,3,\cdots,NN \qquad i,j = x,y,z \tag{5}$$

where the integral terms represent the coefficient matrices and the load vectors, the brace $\{\cdot\}$ terms represent the column vectors of the unknown variable φ and its time derivatives, R is the region of interest with boundary B, and n_j is the component of the outward unit vector $\boldsymbol{n}$, which is normal to the boundary B, in the j direction.

To discretize the time derivative terms in equation (4), the finite difference scheme with a time weighting factor ω is employed. At each time step, the incremental Picard scheme with a nonlinear iteration parameter Ω is then adopted in order to solve the nonlinear problem associated with changes in the unsaturated hydraulic properties (i.e. S_w, dS_w/dh, and K_r) with the pressure head h. To achieve numerical stability, ω is set equal to 1.0 (implicit backward time stepping), and Ω is set equal to 0.25 (under-relaxation) in this paper.

Based on the finite element method described in this section, a general multidimensional numerical model, named COWADE123D (Kim, 1995), has been developed to solve the fully coupled poroelastic governing equations (1) and (2). This numerical model has been successfully verified for its accuracy and applied to a variety of fully coupled hydrogeomechanical phenomena (Kim *et al.*, 1997; Kim and Parizek, 1997; Kim and Parizek, 1999a; Kim and Parizek, 1999b; Kim, 2000).

4. Model Application

Using the fully coupled hydrogeomechanical model developed in the preceding section, a series of steady-state numerical simulations is performed for a straight slope composed of silty soil (silt) and inclined 26.6 ° (2:1 slope) under two different rainfall (precipitation) rates. As shown in Figure 1, the cross section of the slope (40 m × 40 m) is taken as a two-dimensional vertical system with a unit length (1 m) assuming plane strain in the y direction (i.e. perpendicular to the figure). The slope also has a 60-m-wide flat foundation on the slope crest.

The rainfall rates used in this modeling correspond to those during dry and wet seasons between 1990 and 1999 in Seoul, Korea. In Seoul, for the ten years, the driest month (dry season) is January with the rainfall rate of 6.13×10^{-9} m/sec while the wettest month (wet season) is August with the rainfall rate of 4.62×10^{-7} m/sec (Korea Meteorological Administration, 1990-1999).

The hydraulic and mechanical properties of the silt are as follows (van Genuchten, 1980; Guymon, 1994; Lambe and Whitman, 1969; Bardet, 1997): n = 0.46, $K_{sat\,ij} = 6.94 \times 10^{-7}\ \delta_{ij}$ m/sec, ν = 0.33, $E = 1.10 \times 10^{7}$ N/m^2, $\rho_s = 2.67 \times 10^{3}$ kg/m^3, α_c = 1.00, S_{wr} (residual water saturation) = 7.39×10^{-2}, α_{VG} (van Genuchten's parameter) = 1.6 m^{-1}, n_{VG} (van Genuchten's parameter) = 1.37, ϕ' (effective angle of internal friction) = 30 °, c' (effective cohesion) = 1.00×10^{4} N/m^2, and T_o (effective tensile strength) = 0.00 N/m^2.

The system is discretized into 592 isoparametric 4-node quadrilateral elements with 646 nodes. Along the left-hand side at x = 0 m, a no-flow boundary condition and a no-horizontal displacement boundary condition are applied considering the symmetry, but vertical displacement is allowed. The same boundary conditions are also applied along the right-hand side at x = 100 m. The impermeable bottom surface at z = 0 m is fixed vertically, but it is free to move horizontally. The top slope surface is free to move both vertically and horizontally, and it is treated as permeable by applying a variable rainfall-infiltration-seepage boundary condition to take into account infiltration and seepage along the slope surface under rainfall. The numerical implementation of this mixed-type

boundary condition was described in detail by Huyakorn *et al.* (1986), Kim (1995), and others.

The numerical simulation results show certain differences in the hydrogeomechanical responses of the slope to those two different rainfall rates. In Figure 1, the spatial distributions of pressure head, hydraulic head, and Darcy velocity in the slope during the dry season are shown on the left column and are compared with those in the slope during the wet season on the right column. The pressure head (pore water pressure) and hence the total hydraulic head increase as the rainfall rate increases. As a result, the groundwater table rises, the unsaturated zone is reduced, the seepage face expands from the slope toe toward the slope crest, and Darcy velocity increases along the seepage face. In Figure 2, the spatial distributions of displacement vector, factor of safety, and potential failure index in the slope during the dry season are shown on the left column and are compared with those in the slope during the wet season on the right column. The horizontal displacement increases, and the vertical displacement decreases as the rainfall rate increases. As a result, the overall deformation intensifies toward the slope toe, and the unstable zone, in which the factor of safety is less than one, propagates from the slope toe toward the slope crest and becomes thicker near the slope toe. The spatial distributions of factor of safety and potential failure index also suggest that the potential failure may initiate from the slope toe as the rainfall rate increases, and the tension failure is likely to occur as much as the shear failure along the slope surface near the slope toe.

5. Conclusions

A fully coupled hydrogeomechanical numerical model is presented to analyze rainfall impacts on groundwater flow in slopes and slope stability. This numerical model is developed based on the poroelastic governing equations for groundwater flow in deforming variably saturated porous geologic media and the Galerkin finite element method. Using the model developed, a series of numerical experiments is performed under two different rainfall rates. The numerical simulation results show that the overall hydromechanical slope stability deteriorates as the rainfall rate increases. The numerical simulation results also suggest that the potential failure may initiate from the slope toe as the rainfall rate increases, and the tension failure is likely to occur as much as the shear failure along the slope surface near the slope toe. Further numerical studies under various situations and field applications are recommended to arrive at more general conclusions concerning the rainfall impacts on groundwater flow in variably saturated slopes and slope stability.

Acknowledgments

This research was supported in part by the Korea Science and Engineering Foundation (KOSEF) under grant 98-0703-0101-5. Partial support was also provided by the Korea Institute of Geology, Mining and Materials (KIGAM). These supports are gratefully acknowledged.

References

1. Bardet, J. P. (1997), *Experimental Soil Mechanics*, 582 pp., Prentice Hall, Upper Saddle River, New Jersey.
2. Biot, M. A. (1941), "General theory of three-dimensional consolidation", *Journal of Applied Physics*, Vol. 12, No. 2, pp. 155-164.
3. Cai, F., Ugai, K., Wakai, A. and Li, Q. (1998), "Effects of horizontal drains on slope stability

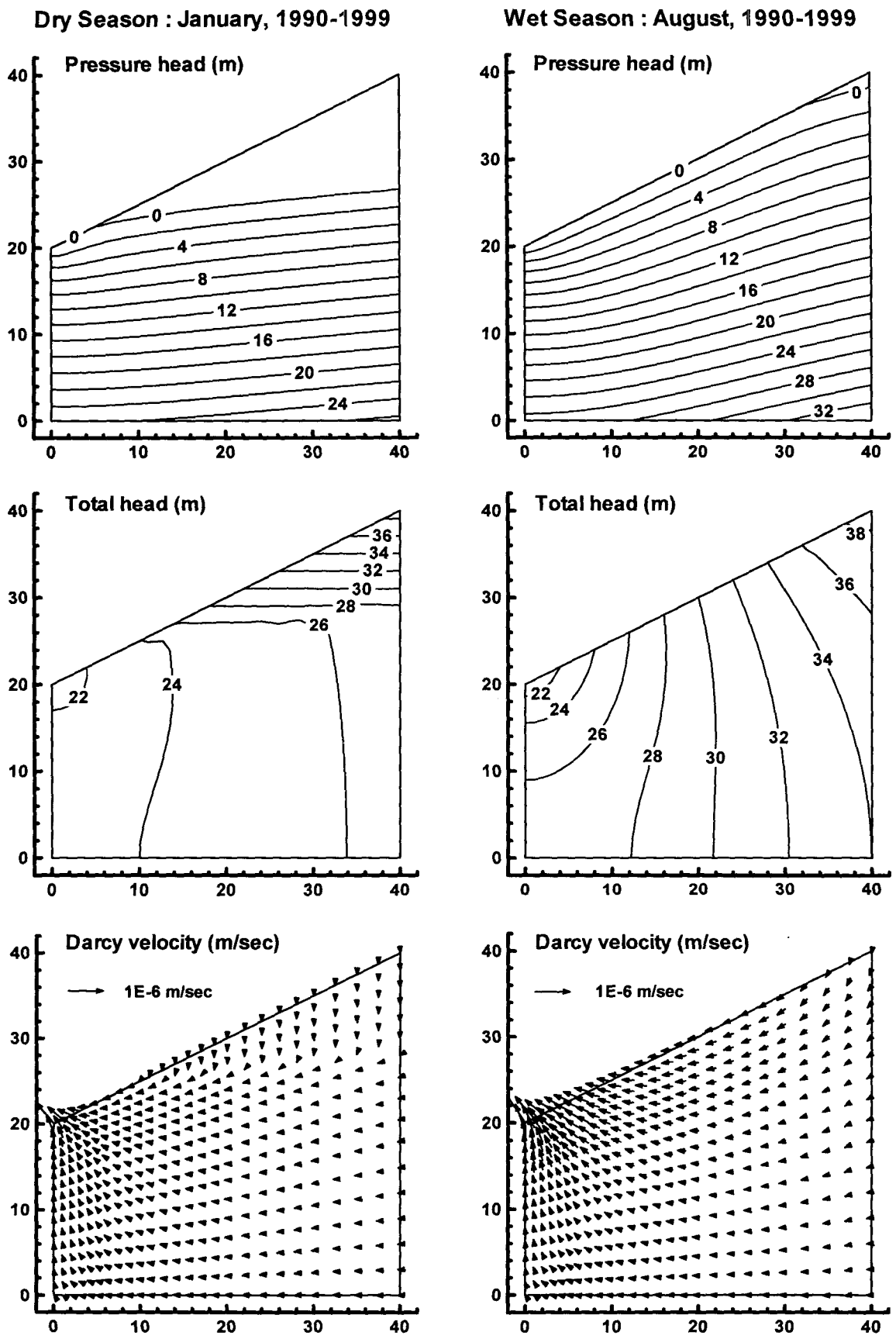

Figure 1. Spatial distributions of pressure head, total head, and Darcy velocity during the dry season (left column) and the wet season (right column) between 1990 and 1999.

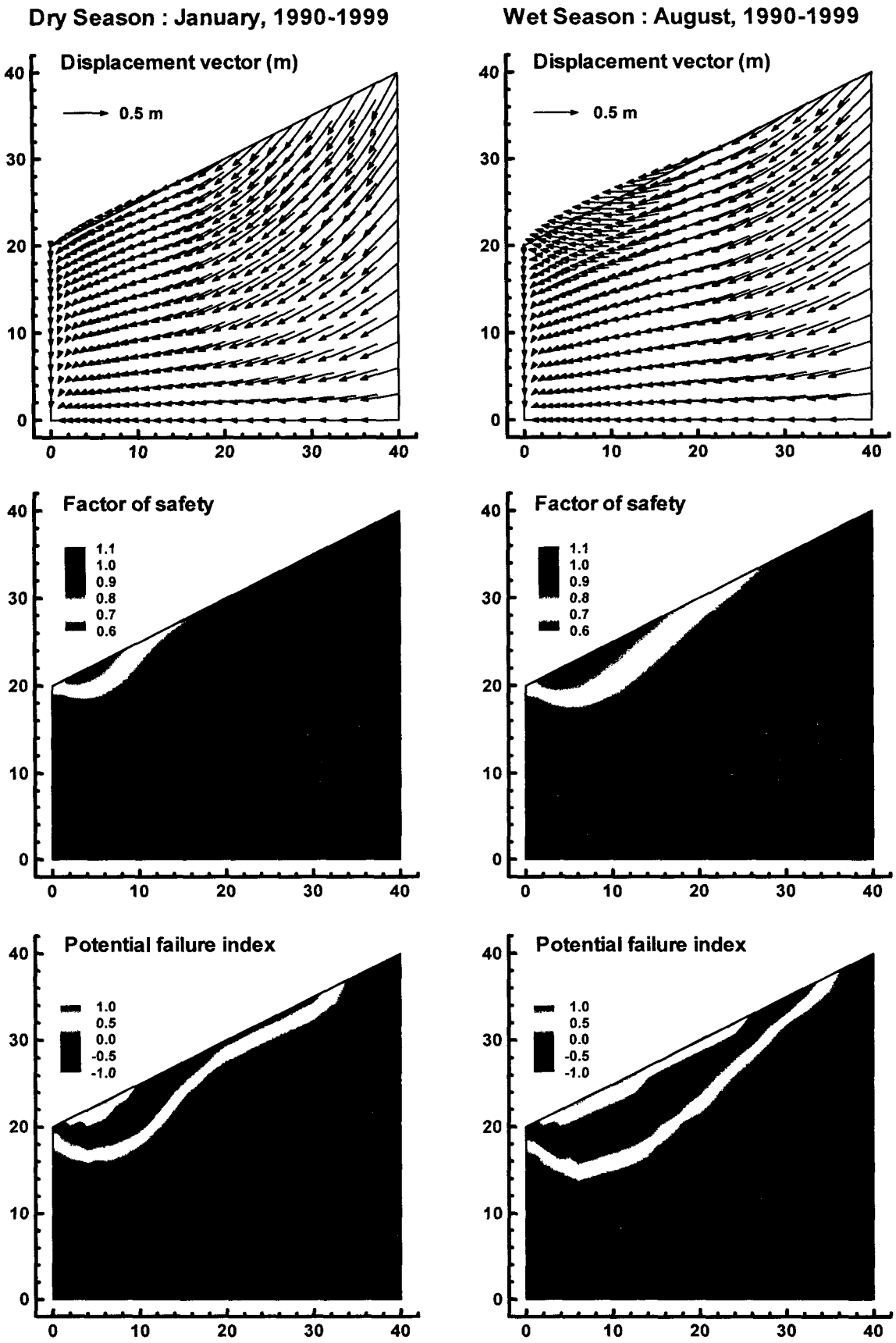

Figure 2. Spatial distributions of displacement vector, factor of safety, and potential failure index during the dry season (left column) and the wet season (right column) between 1990 and 1999.

under rainfall by three-dimensional finite element analysis", *Computers and Geotechnics*, Vol. 23, No. 4, pp. 255-275.
4. Fourie, A. B., Rowe, D. and Blight, G. E. (1999), "The effect of infiltration on the stability of the slopes of a dry ash dump", *Géotechnique*, Vol. 49, No. 1, pp. 1-13.
5. Guymon, G. L. (1994), *Unsaturated Zone Hydrology*, 210 pp., Prentice Hall, Englewood Cliffs, New Jersey.
6. Huyakorn, P. S., Springer, E. P., Guvanasen, V. and Wadsworth, T. D. (1986) "A three-dimensional finite-element model for simulating water flow in variably saturated porous media", *Water Resources Research*, Vol. 22, No. 13, pp. 1790-1808.
7. Istok, J. (1989), *Groundwater Modeling by the Finite Element Method, Water Resources Monograph Series*, Vol. 13, 495 pp., American Geophysical Union, Washington, DC.
8. Iverson, R. M. and Reid, M. E. (1992), "Gravity-driven groundwater flow and slope failure potential, 1. Elastic effective-stress model", *Water Resources Research*, Vol. 28, No. 3, pp. 925-938.
9. Kim, J. M. (1995), COWADE123D: A finite element model for fully coupled saturated-unsaturated water flow in deforming one-, two-, and three-dimensional porous and fractured media, *Technical Report HGL-1995-9*, 254 pp., Hydrogeology Laboratory, Department of Geosciences, Pennsylvania State University, University Park, Pennsylvania.
10. Kim, J. M. (2000), "A fully coupled finite element analysis of water-table fluctuation and land deformation in partially saturated soils due to surface loading", *International Journal for Numerical Methods in Engineering*, in press.
11. Kim, J. M. and Parizek, R. R. (1997), "Numerical simulation of the Noordbergum effect resulting from groundwater pumping in a layered aquifer system", *Journal of Hydrology*, Vol. 202, Nos. 1-4, pp. 231-243.
12. Kim, J. M. and Parizek, R. R. (1999a), "Three-dimensional finite element modelling for consolidation due to groundwater withdrawal in a desaturating anisotropic aquifer system", *International Journal for Numerical and Analytical Methods in Geomechanics*, Vol. 23, No. 6, pp. 549-571.
13. Kim, J. M. and Parizek, R. R. (1999b), "A mathematical model for the hydraulic properties of deforming porous media", *Ground Water*, Vol. 37, No. 4, pp. 546-554.
14. Kim, J. M., Parizek, R. R. and Elsworth, D. (1997), "Evaluation of fully-coupled strata deformation and groundwater flow in response to longwall mining", *International Journal of Rock Mechanics and Mining Sciences*, Vol. 34, No. 8, pp. 1187-1199.
15. Korea Meteorological Administration (1990-1999), *Climatological Data: Seoul, Korea.*
16. Lambe, T. W. and Whitman, R. V. (1969) *Soil Mechanics, SI Version*, 553 pp., John Wiley and Sons, New York.
17. Lewis, R. W. and Schrefler, B. A. (1998), *The Finite Element Method in the Static and Dynamic Deformation and Consolidation of Porous Media*, second edition, 492 pp., John Wiley and Sons, New York.
18. Ng, C. W. W. and Shi, Q. (1998), "A numerical investigation of the stability of unsaturated soil slopes subjected to transient seepage", *Computers and Geotechnics*, Vol. 22, No. 1, pp. 1-28.
19. Reid, M. E. and Iverson, R. M. (1992), "Gravity-driven groundwater flow and slope failure potential, 2. Effects of slope morphology, material properties, and hydraulic heterogeneity", *Water Resources Research*, Vol. 28, No. 3, pp. 939-950.
20. van Genuchten, M. Th. (1980), "A closed-form equation for predicting the hydraulic conductivity of unsaturated soils", *Soil Science Society of America Journal*, Vol. 44, No. 5, pp. 892-898.